Interplay of Troponin- and Myosin-Based Pathways of Calcium Activation in Skeletal and Cardiac Muscle: The Use of W7 as an Inhibitor of Thin Filament Activation

Bishow B. Adhikari and Kuan Wang
Muscle Proteomics and Nanotechnology Section, Laboratory of Muscle Biology, National Institutes of Arthritis and Musculoskeletal and Skin Diseases, National Institutes of Health, Bethesda, Maryland

ABSTRACT To investigate the interplay between the thin and thick filaments during calcium activation in striated muscle, we employed *n*-(6-aminohexyl) 5-chloro-1-napthalenesulfonamide (W7) as an inhibitor of troponin C and compared its effects with that of the myosin-specific inhibitor, 2,3-butanedione 2-monoxime (BDM). In both skeletal and cardiac fibers, W7 reversibly inhibited ATPase and tension over the full range of calcium activation between pCa 8.0 and 4.5, resulting in reduced calcium sensitivity and cooperativity of ATPase and tension activations. At maximal activation in skeletal fibers, the W7 concentrations for half-maximal inhibition (K_I) were 70–80 μM for ATPase and 20–30 μM for tension, nearly >200-fold lower than BDM (20 mM and 5–8 mM, respectively). When W7 (50 μM) and BDM (20 mM) were combined in skeletal fibers, the ATPase and tension-pCa curves exhibited lower apparent cooperativity and maxima and higher calcium sensitivity than expected from two independent activation pathways, suggesting that the interplay between the thin and thick filaments varies with the level of activation. Significantly, the inhibition of W7 increased the ATPase/tension ratio during activation in both muscle types. W7 holds much promise as a potent and reversible inhibitor of thin filament-mediated calcium activation of skeletal and cardiac muscle contraction.

INTRODUCTION

Calcium activation of contraction and its regulation in vertebrate striated muscle involve both the thin and the thick filaments. Initiation of activation is triggered by the binding of calcium to troponin C (TnC), followed by conformational changes and movement of the troponin/tropomyosin complexes of the thin filament that render the force-generating interactions between actins of the thin filaments and myosin motors of the thick filaments. The interaction between the two filament systems is thought to be interdependent, with each system simultaneously responding to and influencing the other system (Gordon et al., 2000). The interplay of the two filaments has been examined experimentally by two general approaches: 1), preferential extraction and reconstitution or exchange with modified or analogous proteins; and 2), the use of specific inhibitors (usually small chemical compounds) to perturb or inhibit protein interactions. In the present study, we have employed inhibitors that preferentially target either the TnC in the thin filament or the myosin heads in the thick filament, to gain further understanding of the relative contribution and interdependence of the activation processes of the thin and the thick filaments.

To inhibit the thin filament activation via TnC, we utilized *n*-(6-aminohexyl) 5-chloro-1-napthalenesulfonamide (W7) as an inhibitor, a compound originally developed as a potent and specific inhibitor of calmodulin (CaM) function (Hidaka et al., 1980). W7 is known to bind specifically and with high affinity to CaM ($K_d = 11$ μM at 25°C) and to TnC ($K_d = 25$ μM at 25°C), but not to actin, myosin, or tropomyosin (Tm) (Hidaka et al., 1980). W7 binds to the hydrophobic pocket formed by the EF hands within each domain of CaM and competes directly with the binding of CaM-dependent enzymes (Osawa et al., 1998). Although W7 binds to TnC in solution, its potential ability to inhibit muscle activation was curiously not borne out by previous work in skinned rabbit psoas fibers (Ogawa and Kurebayashi, 1989). We found that, contrary to this early work, W7 indeed is a potent and reversible inhibitor of calcium activation in skinned fibers from both rabbit skeletal and mouse cardiac muscles.

The inhibitory effect of W7 in skeletal fibers was compared with that of 2,3-butanedione 2-monoxime (BDM), a widely used inhibitor that targets actively cycling myosin heads (Herrmann et al., 1992; McKillop et al., 1994) and inhibits ATPase uncompetitively by stabilizing the posthydrolysis state before the force-generating isomerization state (McKillop et al., 1994; Regnier et al., 1995; Tesi et al., 2002; Zhao et al., 1995; Zhao and Kawai, 1994). The combined use of W7 and BDM offers an opportunity to examine the degree and the mechanism of coupling between the thin and the thick filaments during calcium activation of contraction. To

Submitted February 7, 2003, and accepted for publication August 18, 2003.

Address reprint requests to Kuan Wang, PhD, Building 50, Rm. 1140, Laboratory of Muscle Biology, NIAMS, National Institutes of Health, 9000 Rockville Pike, Bethesda, MD 20892. Tel.: 301-496-4097; Fax: 301-402-0009; E-mail: wangk@exchange.nih.gov.

Bishow B. Adhikari's present address is Dept. of Bioengineering, University of Washington, Seattle, WA 98195.

Abbreviations used: TnC, troponin C; CPK, creatine phosphokinase; SL, sarcomere length; CaM, calmodulin; KPr, potassium propionate; LDH, L-lactic dehydrogenase; PEP, phosphoenolpyruvate; PK: pyruvate kinase; EGTA, ethylene glycolbis(β-amino-ethyl ether)-*n*,*n*,*n*′,*n*′ tetraacetic acid; RLC, regulatory light chain; ELC, essential light chain; BES, *n*,*n*-bis[2-Hydroxyethyl]-2-aminoethane-sulfonic acid.

0006-3495/04/01/359/12 $2.00

assess the inhibition in rabbit skeletal and mouse cardiac muscle, we measured the activations of ATPase and tension simultaneously as calcium concentration was increased continuously from pCa 8.0 to 4.5. Comparison of the extent of inhibition and the coupling between ATPase and tension were facilitated by subjecting the same samples to several cycles of activation/relaxation in the presence of the inhibitors. The ATPase- and tension-pCa curves were fitted with the Hill equation to determine the cooperativity and calcium sensitivity of activation (Donaldson and Kerrick, 1975).

We report that W7 is a potent and reversible inhibitor of thin filament-mediated calcium activation in skeletal and cardiac fibers. W7 reversibly reduces the ATPase, tension and the tension cost (ATPase/tension ratio) over the entire range of activation by calcium. The comparison of W7 and BDM inhibitions in skeletal and cardiac fibers revealed the interdependence of thin- and thick-filament-based activations in each muscle type.

EXPERIMENTAL PROCEDURES

Sample preparation

Bundles of skinned rabbit psoas fibers were prepared from adult white New Zealand rabbits (~2 kg) as described previously (Adhikari and Wang, 2001). Skinned fiber bundles from mouse papillary were prepared according to Fewell et al. (1998). After euthanasia of mice by CO_2 and cervical dislocation, the heart was removed and immediately immersed in solution A (5.37 mM Na_2ATP, 30 mM phosphocreatine, 5 mM K-EGTA, 20 mM BES, 7.33 mM $MgCl_2$, 0.12 mM $CaCl_2$, 10 mM DTE, 1% (v/v) protease inhibitor cocktail (P-8340, Sigma, St. Louis, MO), 30 mM BDM, and 32 mM potassium methanesulfonate, pH 7.0). Uniform sections of left ventricular papillary tissues (~0.5 mm × 2–3 mm) were dissected and skinned in solution B (5.5 mM Na_2ATP, 5 mM K-EGTA, 20 mM BES, 6.13 mM $MgCl_2$, 0.11 mM $CaCl_2$, 10 mM DTE, the protease inhibitor cocktail, 121.8 mM potassium methanesulfonate at pH 7.0, and 50% glycerol and 0.5% (v/v) Triton X-100) for 12 h, and stored in solution B without detergent at –20°C until use.

Single rabbit psoas fibers were dissected from bundles under relaxing solution (Table 1) and glued to aluminum T-clips (~0.5 × 2 mm) using an octyl-formulated cyanoacrylate glue (Nexaband S/C, Closure Medical Corporation, Raleigh, NC) at a length of ~1.5–2 mm and attached via holes in the T-clips. The attachment was via tweezers without the T-clips for the simultaneous pCa-ATPase and pCa-tension measurements (Fig. 1 *A*). Mice papillary tissues were dissected under solution A to get thin and uniform fiber bundles (~100–150 μm × 2 mm) and subjected to a further skinning for 4–6 h in solution B. All calcium activation experiments were carried out at 20°C at a preset sarcomere length (SL) = 2.2 μm.

TABLE 1 Solutions used for mechanical studies

	Rigor	Relaxing	Rx-NADH	Activating	Act-NADH
Imidazole (mM)	10	10	10	10	10
K_2-EGTA (mM)	12	12	12	0	0
K_2Ca-EGTA (mM)	0	0	0	12	12
Magnesium acetate (mM)	1.3	3.0	3.0	2.5	2.5
KPr (mM)	138	117	127	116	128
Na_2ATP (mM)	0	1.8	1.8	1.8	1.8
DTT (mM)	1	1	1	1	1
CP (mM)	0	5	0	5	0
CPK (units/ml)	0	200	0	200	0
NADH (mM)	0	0	0.4	0	0.4
LDH (units/ml)	0	0	140	0	140
PK (units/ml)	0	0	100	0	100
PEP (mM)	0	0	5	0	5
Leupeptin (μg/ml)	20	20	20	20	20
pH	7.0	7.0	7.0	7.0	7.0
Ionic strength (mM)	180	180	180	180	180
pCa	~8.0	~8.0	~8.0	4.0	4.0
[MgATP] (mM)	0	1.5	1.5	1.5	1.5
[Mg^{2+}] (mM)	1	1	1	1	1

Solution compositions

Solution compositions for the fiber experiments are given in Table 1. Isometric tension and stiffness experiments at pCa 4.0 were carried out with relaxing and activating solutions with ATP-regenerating backup system. Calcium activation experiments were carried out in Rx-NADH and Act-NADH solutions. The concentrations of free Ca^{2+}, free Mg^{2+}, MgATP, and the total ionic strength in these solutions were calculated using the program MaxChelator V1.75 (Chris Patton, Stanford University; http://www.stanford.edu/cpatton/maxc.html, August, 1998). The dissociation constants of metal ion chelators in the solution were taken from Martell and Smith (1974). Calculated solution pCa was routinely verified with calcium selective electrode (Orion Research, Beverly, MA) using calibrated pCa standards (WPI, Sarasota, FL).

Tension and dynamic stiffness measurements

A previously described instrument (Granzier and Wang, 1993) with modifications was used to measure tension and dynamic stiffness (single or sweeps between 1 and 2000 Hz) under isometric conditions. Stiffness refers to the dynamic stiffness determined by the ratio of the amplitudes of tension and percent fiber length resulting from sinusoidal oscillations (0.1% fiber length or ~1 nm per half sarcomere s^{-1}) imposed at one end of fiber through the length transducer. Fiber cross-sectional area was calculated assuming uniform cylindrical diameter from the average of 4–8 measurements taken at equidistant points along fiber axis at a magnification of 400×.

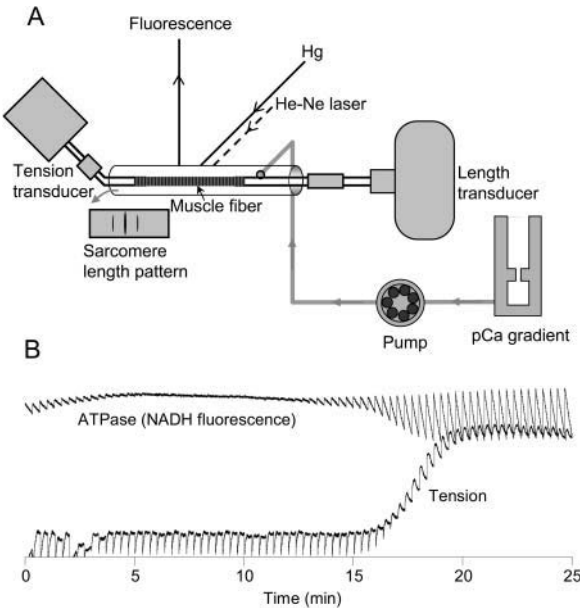

FIGURE 1 Schematic of instrument and an example of raw data obtained during calcium activation of ATPase and tension. (*A*) Single skeletal fiber or a small bundle of cardiac papillary fibers is mounted between two tweezers, one attached to a length controller and the other to a force transducer, inside a cuvette. Solution of varying pCa can be pumped around the sample using a peristaltic pump and a pCa gradient maker that mixes solutions of low and high calcium. For fluorescence measurements, excitation light is focused on the sample, and two detectors, one of each for the signal and the background, are used to collect the resulting fluorescence with appropriate excitation and emission filters. Sarcomere length is measured from diffraction patterns from a He-Ne laser. (*B*) Raw data of NADH fluorescence (ATPase) and tension that are used to construct two calcium activation curves of the same single rabbit psoas fiber.

pCa curves of tension and ATPase

The pCa curves of ATPase and tension for a given fiber from pCa 8.0 to 4.6 at 20°C (Fig. 1 *A*) were determined simultaneously in a commercially available instrument (Scientific Instrument, Heidelberg, Germany), as described previously (Adhikari and Wang, 2001). Typically, multiple cycles of activation, each preceded by a relaxation period, were carried out on the same sample at different inhibitor concentrations to determine the extent and reversibility of the inhibition. Raw data from one of the activation cycles (Fig. 4, *II-Cycle 2*) after treatment and washing of W7 are shown in Fig. 1 *B*. Each spike in the tension and ATPase traces corresponds to the successive perfusions of the sample. The ATPase, given by the rate of decrease of NADH fluorescence between each perfusion, and the tension remain at baseline values until sufficient calcium is available to activate the fiber and trigger a rapid response to saturating values at higher calcium (lower pCa). ATP turnover per myosin head s^{-1} were determined by calibration of fluorescence intensity with known concentrations of NADH, assuming myosin head concentration of 150 μM (Bagshaw, 1993).

The pCa curves of ATPase and tension, normalized to the maximum values in the absence of inhibitors either before or after treatment, were fitted using nonlinear routines (MathCAD 8.0, MathSoft, Cambridge, MA) with the following equation,

$$Y = Y_{max}[Ca^{2+}]^n/(\alpha_C K_M^n + \alpha_U[Ca^{2+}]^n), \quad (1)$$

which can be written as

$$y = y_{max}/(\alpha_U + \alpha_C 10^{n(pCa-K_M)}), \quad (2)$$

where y_{max} and K_M denote, respectively, the maximum activation (100%) and the pCa at which activation is at the half-maximum (pK) for the pCa curves without the inhibitors. For all pCa curves, n is the slope and represents a measure of the cooperativity of activation. In the presence of an inhibitor, the coefficients, α_C, α_U (≥ 1), determine the decreases in the pK (as a measure of competitive inhibition) and the maximal activation (as a measure of uncompetitive inhibition), respectively. The pK is given by (K_M-log (α_C)/n) and the relative maximal activation is given by 100%/α_U. In the absence of inhibitor, α_C, $\alpha_U = 1$, and Eq. 2 then reduces to the Hill equation used previously for the analysis of pCa curves (Donaldson and Kerrick, 1975).

RESULTS

Inhibition of tension and stiffness in skeletal fibers by W7 at pCa 4.0

When increasing concentrations of W7 (0–300 μM) were added to a skinned single rabbit psoas fiber undergoing isometric contraction at pCa 4.0 at 20°C, tension declined incrementally with the added W7, reaching 4% of maximal values without W7 at 300 μM (Fig. 2 *A*). Subsequent washing to remove free W7 restored the tension to the same level as untreated control fibers (Fig. 2 *A*), with a slow decline of maximal isometric tension over the time course of the experiments. The inhibition was stable for at least 16 min (not shown), repeatable (e.g., Fig. 2, *B* and *C*), and independent of the sequence of the treatments (Fig. 2, *A* and *B*). Prior activation was not necessary for this effect, since activation in the presence of W7 produced the same degree of inhibition as that of W7 treatment after activation (Fig. 2, *B* and *C*).

The inhibition of tension (at 20°C and 5°C) and dynamic stiffness (20°C) as a function of W7 concentration is shown in Fig. 3. The decline in tension at both temperatures was rapid initially, dropping to 30% between 0 and 50 μM, but became much more moderate at higher concentrations. W7 inhibited tension more effectively at 20°C than 5°C. Its inhibition of dynamic stiffness (at 96 Hz, 440 Hz, and 2 kHz) followed closely and appeared proportionally with that of tension (*inset*, Fig. 3). Simple hyperbolic curves fit the tension data reasonably well, yielding concentrations for half-maximal inhibition ($K_{I\text{-}Tension}$) of 22 and 32 μM,

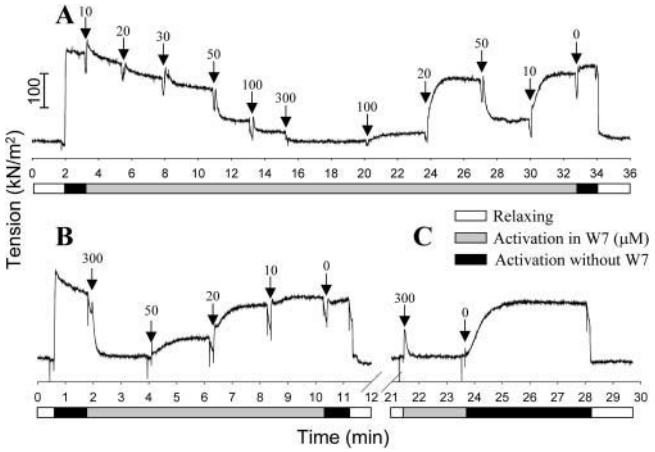

FIGURE 2 The reversible inhibition of isometric tension of rabbit psoas fibers by W7 at pCa 4.0. (*A*) A single fiber, initially under relaxation, was activated at pCa 4.0 and subjected to increasing and decreasing concentrations of W7 before another final relaxation. The numbers above the trace indicate the concentration of W7 in μM. (*B*) Another fiber was treated with 300 μM W7 after activation, which resulted in tension levels approaching the relaxing value, and then treated with 50, 20, and 10 μM W7 with a corresponding recovery of tension. Subsequently, when the fiber was treated with relaxing solution the tension returned to relaxing values. (*C*) The same fiber from *B* after 10 min relaxation was activated first in 300 μM W7; then without W7; then finally relaxed.

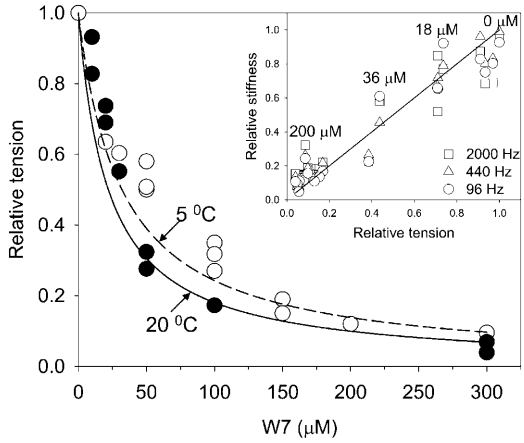

FIGURE 3 Isometric tension and stiffness at pCa 4.0 of rabbit psoas fibers as a function of W7 concentration. Tension was normalized to values obtained without W7. The data were obtained from four experiments at 20°C (*solid symbols*) and three experiments at 5°C (*unfilled symbols*). The solid lines are drawn to fit the tension data using an equation of a hyperbola with half-maximal values ($K_{\text{I-Tension}}$) of 22 μM at 20°C and 32 μM at 5°C. Inset shows the proportionality between tension and stiffness (2000, 440, and 96 Hz) at the indicated W7 concentrations at 20°C.

respectively, at 20 and 5°C (Fig. 2). The $K_{\text{I-Tension}}$ at 20°C observed here is close to the reported dissociation constant of 25 μM between W7 and TnC measured in solution at 25°C (Hidaka et al., 1980).

Inhibition of calcium activation of ATPase and tension in skeletal fibers by W7

W7 greatly reduced the magnitudes and calcium sensitivities of ATPase and tension over the entire pCa range between 7.0 and 4.8. At 300 μM, W7 abolished tension nearly completely; however, residual ATPase (~17%) between pCa 5.8 and 5.0 remained (Fig. 4, *I-Cycle 1*). When the concentration was reduced in successive activation cycles, ATPase and tension recovered correspondingly, with the curves at 0 μM returning to the steep and high amplitude curves typical of the untreated fibers (Fig. 4, *untreated*). The maximum activations of ATPase and tension were, respectively, 39 and 11% at 100 μM and 83 and 58% at 20 μM. It is interesting that ATPase is more sensitive to calcium activation, with a pK that is higher by ~+0.12 than that of the tension pCa curves without W7 (Fig. 4, *untreated*). This difference was widened to +0.2 to 0.4 at higher concentrations of W7 (Fig. 4). From the variations of maximal ATPase and maximal tension against W7, $K_{\text{I-ATPase}}$, and $K_{\text{I-Tension}}$ were determined as ~75 μM and ~25 μM, respectively.

A closer examination of the deviations of experimental and fitted ATPase-pCa curves revealed the likely presence of three component curves (Fig. 4). The first component (*l*) was observed at the onset of activation between pCa 6.6 and 5.9 (*bracket*, Fig. 4, *I-Cycle 2*). This leading component (*l*), which peaks at ~20% of the maximal ATPase value, was frequently, but not always, inhibited by W7. The second and major component comprised ~80% of the total maximal ATPase observed between pCa 5.9 and 5.0 and was W7-sensitive (*fitted solid curve*, Fig. 4, *I-Cycle 2*). A third, trailing component (*t*) was observed between pCa 5.6 and 5.0 that accounted for ~17% of the maximal ATPase and was uninhibited by high concentrations of W7 to at least 300 μM (*bracket*, Fig. 4, *II-Cycle 1*).

Inhibition of cardiac muscle activation by W7

Since TnC-mediated calcium activation is analogous in skeletal and cardiac muscle, we evaluated whether W7 has a similar effect on mouse papillary muscle. As in skeletal fibers, the inhibition of activations of ATPase and tension by W7 was reversible and characterized by reduced maxima and reduced calcium sensitivities. However, cardiac fibers appeared to be more resistant to W7, with a $K_{\text{I-ATPase}}$ of ~80 μM and $K_{\text{I-Tension}}$ of ~25 μM.

The maximal ATPase and tension in the same papillary fiber bundle were 48 and 25% at 100 μM (Fig. 5, *Cycle 2*); 58 and 40% at 25 μM (Fig. 5, *Cycle 3*); and finally, after washing, restored to 80 and 70% at 0 μM (Fig. 5, *Cycle 4*).

In the absence of W7 (Fig. 5, *Cycle 1*), the ATPase and tension-pCa curves nearly coincided, with a pK at 5.4 (cf. Allen et al., 2000; Wang et al., 1999). Closer examination of this and other curves indicated that ATPase curves frequently led the tension curves by a small but detectable

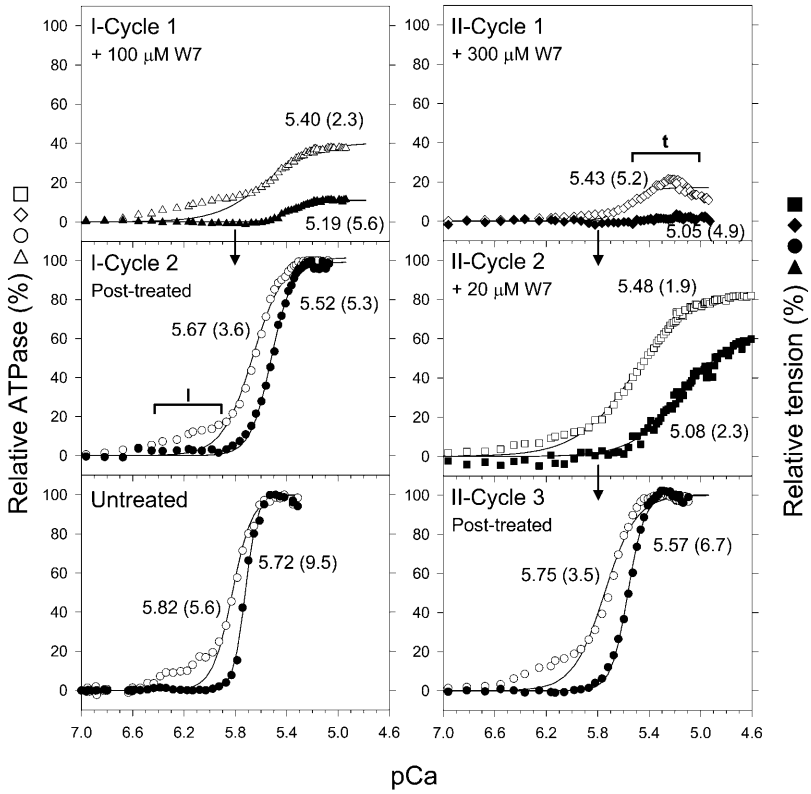

FIGURE 4 The reversible inhibition of calcium activation of ATPase and tension of single rabbit psoas fibers by W. The pCa curves of ATPase (*unfilled symbols*) and tension (*solid symbols*) from two adjacent sections (*I* and *II*) of a single fiber are plotted against the solution pCa. Multiple activation cycles, each preceded by a period of relaxation, were carried on two adjacent sections of a single fiber in the presence of the indicated concentrations of W7. The activation sequences were 100 μM (*I-Cycle 1*) and 0 μM (*I-Cycle 2*) in the first fiber section, and 300 μM (*II-Cycle 1*), 20 μM (*II-Cycle 2*), and 0 μM (*II-Cycle 3*) in the second fiber section. The data were normalized to the curves at 0 μM W7 in each set. The fitted values of midpoint (*pK*) and slope (*n*, in parentheses) are given next to each curve. An example of ATPase/force-pCa curves from an untreated fiber is shown for comparison. The brackets (*l* for leading component and *t* for trailing component) indicate the components of ATPase that are not accompanied by significant levels of tension.

difference of 0.03 pCa unit (Fig. 5, *Cycle 1*). This lead was significantly widened in W7 treated fibers, to +0.16 at 100 μM (Fig. 5, *Cycles 2–4*). Subsequent washing of treated fibers did little to narrow the lead, despite the restoration of ATPase and tension. Interestingly, the leading ATPase component of skeletal fibers, activated between pCa 6.6 and 5.8, was absent in cardiac fibers (Fig. 5).

Alteration of calcium activation in skeletal fibers by W7 and BDM

We next compared the W7 inhibition with BDM in rabbit psoas fibers to explore whether the combined use of W7 and BDM could provide insights on the interplay of the thin filament- and thick filament-based pathways of calcium activation. Fig. 6 shows the results of calcium activation of

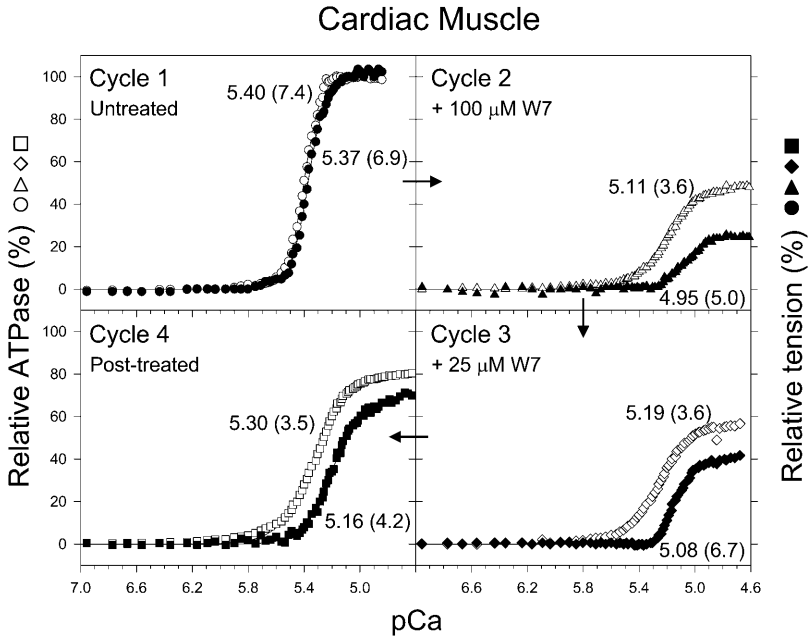

FIGURE 5 The reversible inhibition of calcium activation of ATPase and tension by W7 in mouse heart fibers. All activation curves were obtained sequentially from the same sample, after relaxation of muscle between each activation, in the following order: without W7 (*Cycle 1*), with 100 μM W7 (*Cycle 2*), with 25 μM W7 (*Cycle 3*), and finally again after washing W7 (*Cycle 4*). The data were normalized to the curves obtained in the first activation cycle without W7 (*Cycle 1*). The fitted values of pK and *n* (in parentheses) are given next to each curve.

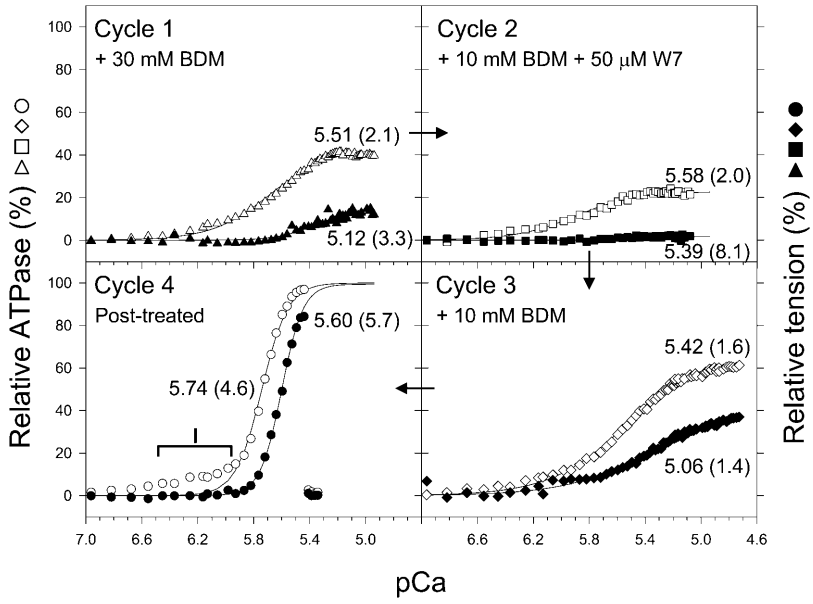

FIGURE 6 The inhibition of calcium activation of tension and ATPase of a rabbit psoas fiber by BDM and by BDM and W7. All activation curves were obtained sequentially in the same fiber, after relaxation of sample between each activation, in the following order: 30 mM BDM (*Cycle 1*), 10 mM BDM plus 50 μM W7 (*Cycle 2*), 10 mM BDM (*Cycle 3*), and finally without BDM and W7 (*Cycle 4*; note that the fiber broke near the maximum activation). The data were normalized to the curves without BDM and W7 (*Cycle 4*; *l* over bracket indicates the leading component of ATPase as in Fig. 4). Fitted values of pK and *n* (in brackets) are given next to each curve.

a fiber treated sequentially with BDM and/or W7 in four cycles. The maximal ATPase and tension were diminished to 40 and 12%, respectively, in 30 mM BDM, with the tension inhibition comparable to previous studies (Martyn et al., 1999). Based on such curves, $K_{\text{I-ATPase}}$ and $K_{\text{I-Tension}}$ of BDM were 20 mM and 5–8 mM, respectively (data not shown). In 10 mM BDM and 50 μM W7, tension maximum was reduced to nearly zero (1.7%) whereas the ATPase maximum was 22%. These values were comparable to the inhibition observed in 300 μM W7 (Fig. 4) but significantly lower than those in 30 mM BDM. Upon reactivation of the same fiber in 10 mM BDM, the maximal ATPase and tension returned to 60 and 35%, respectively. When the fiber was washed to remove free W7 and BDM, the activations approached untreated levels. Interestingly, the leading component of ATPase activation between pCa 6.6 and 5.9 (bracketed in Fig. 4, *I-Cycle 2*; Fig. 6, *Cycle 4*), which was inhibited by W7 (Fig. 4, *I-Cycle 1*, and *II-Cycles 1* and *2*), was also reduced by BDM (Fig. 6, *Cycles 1* and *3*).

It is significant that the maximal ATPase and tension and their apparent cooperativity to calcium were much lower in W7 plus BDM than in W7 or BDM alone (Fig. 7 *A*). To analyze this difference over the entire range of activation, we calculated theoretical curves on the assumption that two inhibitors act independently, so that the total inhibition is the arithmetic sum of individual curves (normalized to the maximal values of untreated fibers) for each inhibitor. As shown in Fig. 7 *B*, the predicted pCa curves of W7 plus BDM intersected with the experimental curves of W7 plus BDM near pCa ~5.3 for both ATPase (*unfilled symbols* in Fig. 7 *B*) and tension curves (*solid symbols* in Fig. 7 *B*). Thus at pCa >5.3, the two inhibitors appear to interfere with each other to give a higher ATPase and tension than those predicted; at pCa <5.3, the two inhibitors appear to enhance the inhibition, resulting in lower ATPase and tension than those predicted.

The inhibitory effects of W7 and BDM in skeletal fibers were largely reversible. Untreated fibers developed on average 182 ± 5 kN/m^2 tension with ATP turnover rate of 3.5 ± 0.2 s^{-1} per active myosin site at maximal activation (Table 2). This ATP turnover rate is comparable to recently published values (Hilber et al., 2001). After the washing to remove inhibitors, the fibers displayed a slightly lower maximal ATPase (by 14%) and maximal tension (by 5%). In normalized pCa curves, the pK of ATPase and tension decreased by 0.1 and 0.18 pCa units, respectively, with a corresponding drop of *n*-values by ~2 and ~3 (Table 2). These changes are comparable to those of fibers that were taken through two consecutive activation cycles in the absence of inhibitors (data not shown).

Tension cost curves during skeletal and cardiac muscle activation

Tension cost, defined as the ratio of ATPase to tension, both normalized to maximal activation values in the absence of inhibitors, is a useful measure of the efficiency of conversion of chemical energy into mechanical energy of the muscle fiber (e.g., Kushmerick and Krasner, 1982). On the assumption that ATPase is myosin-based under our experimental conditions, the tension cost for untreated skeletal fibers upon activation declined steeply from ~6 at pCa of 5.6/5.7 to a plateau value of 1 below pCa 5.5 (Fig. 8 *A*). The tension cost from pCa 6.6 to 5.7 is undefined, since no force was measurable for this leading component of the ATPase-pCa curves (see above). This tension cost-pCa curve indicates that the coupling between ATPase and force generation at the onset of activation is suboptimal and becomes increasingly

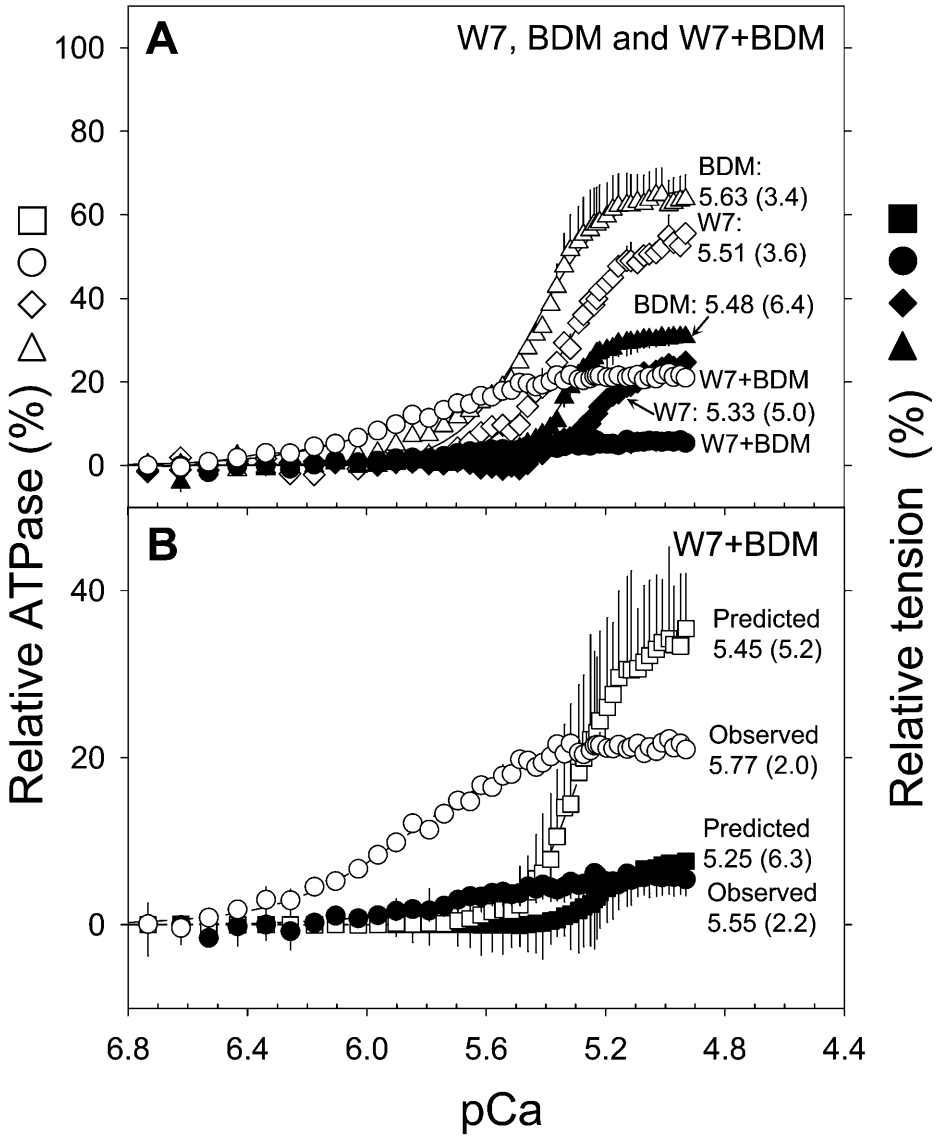

FIGURE 7 Enhancement of inhibition by the combination of 50 μM W7 and 10 mM BDM in single fibers from rabbit psoas muscle. Average ATPase and tension-pCa curves are plotted for 50 μM W7, 10 mM BDM, 50 μM W7, and 10 mM BDM in *A*. The pCa curves of the combined W7 and BDM data are compared with that of the predicted curves based on sums of each inhibition curves in *B*. The fitted values of pK and *n* (in parentheses) for the ATPase and tension curves are given next to each curve. Note the significant drops in cooperativity and maximal values that lead to higher sensitivities when W7 and BDM are combined. The data were obtained from individual activations in 3–4 fibers for each condition.

efficient and reaches a maximum only after this skeletal muscle is fully activated near pCa 5.5 and beyond. Significantly, the tension cost-pCa curve in untreated cardiac fibers was nearly flat over the entire pCa range (Fig. 8 *B*). This curve indicates a constant coupling efficiency between ATPase and tension during activation of cardiac muscles and suggests a qualitative difference of calcium activation between the two muscles.

In the presence of W7 for both muscles, the tension cost increased over the entire pCa range (Fig. 8, *A* and *B*). The tension cost of skeletal fibers in 20 μM W7 was higher than that of the untreated fiber between pCa 5.6 and 4.9. This curve descended gradually from pCa 5.6 toward pCa 4.9 and plateaued to ~2 at pCa 4.9 (Fig. 8 *A*). Similarly, the curve at 100 μM W7 was even higher than 20 μM W7 and plateaued to ~3 (Fig. 8 *A*). In cardiac fibers treated

TABLE 2 The reversibility of W7 and BDM treatment on calcium activation of ATPase and tension in single skeletal fibers

	Untreated fibers			Posttreated fibers		
	Maximum*	pK	Hill (*n*)	Maximum*	pK	Hill (*n*)
ATPase	3.5 ± 0.2	5.83 ± 0.01	6.4 ± 0.6	3.0 ± 0.2	5.73 ± 0.02	4.1 ± 0.3
Tension	182 ± 5	5.75 ± 0.01	9.3 ± 0.4	172 ± 8	5.57 ± 0.02	6.2 ± 0.4

*Fibers were activated without treatment (*untreated fibers*), or treated with both inhibitors, activated, washed, and then reactivated (*posttreated fibers*). ATPase is given as ATP turnover per active site per second and tension is in kN/m^2. Data are averages of individual analyses of five activations in five fibers in each set.

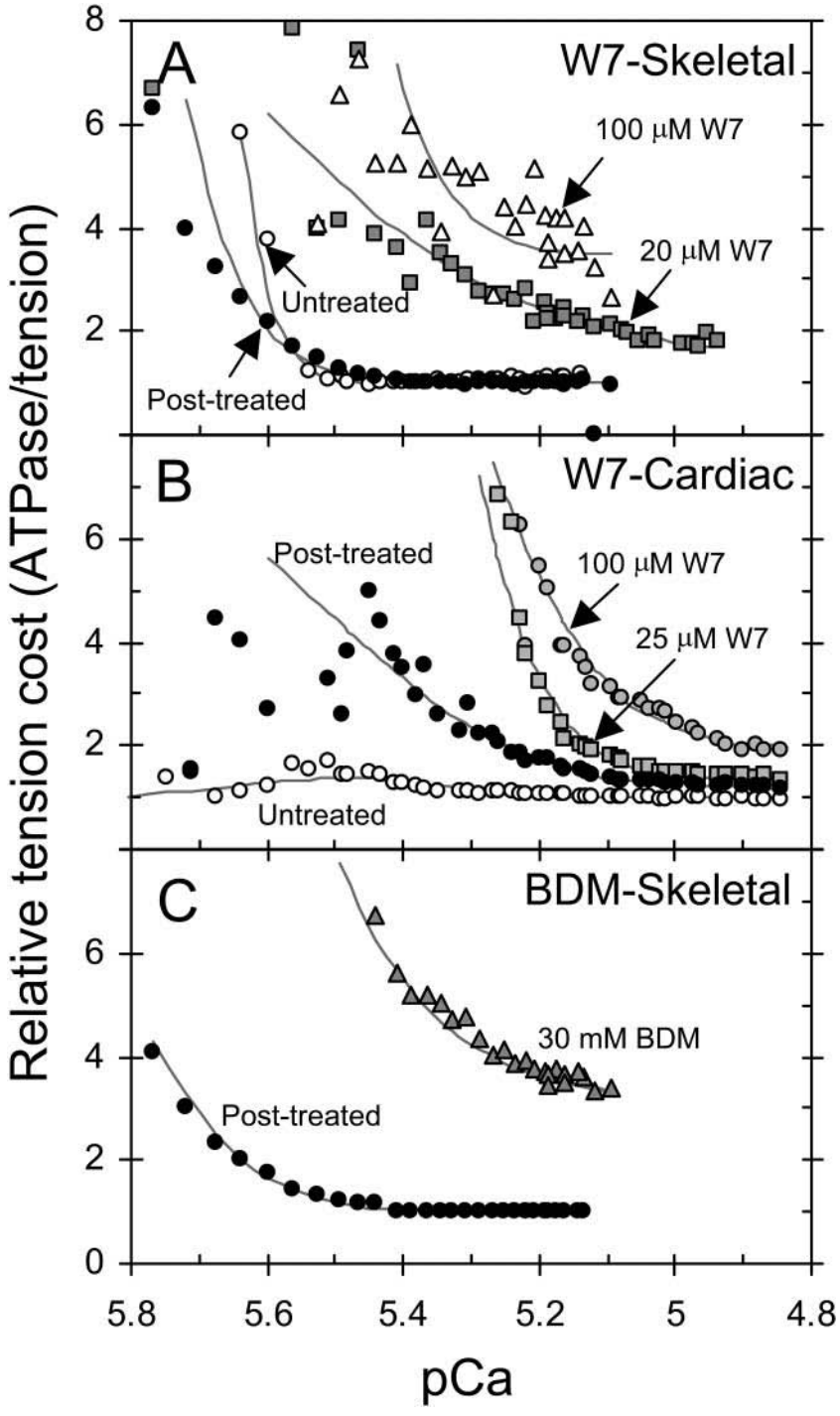

FIGURE 8 Relative tension cost (ATPase/tension) during activation in the presence of W7 and BDM. The ATPase/tension ratios are plotted against the solution pCa for activations of skeletal and cardiac fibers at the indicated concentrations of W7 and BDM. (*A*) W7 inhibition in skeletal fibers; (*B*) W7 inhibition in cardiac fibers; and (*C*) BDM inhibition in skeletal fibers.

with W7, a similar increase in tension cost was observed with increasing concentrations of W7 (Fig. 8 *B*). After washing of treated fibers to remove inhibitors, the tension cost curves recovered completely for the skeletal muscle and significantly for the cardiac muscle (compare untreated and posttreated curves in Fig. 8). The skeletal muscle curve at 30 mM BDM descended from 6 at pCa 5.4 to a plateau at 3 at pCa 5.1 (Fig. 8 *C*). These data indicate that these inhibitors increase the tension cost of contraction over the entire range of pCa for both skeletal and cardiac muscles.

DISCUSSION

W7 as a novel inhibitor of skeletal and cardiac muscle contraction

We have established for the first time that a widely used CaM antagonist, W7, is a potent and reversible inhibitor of

contraction in skeletal and heart muscle fibers. This small, membrane-permeable inhibitor of high potency and reversibility, is expected to be particularly useful, either by itself or in combination with other known inhibitors, such as BDM or the recently reported myosin inhibitor BTS (Cheung et al., 2002), for the fine control of contraction of live muscle fibers. It may also be utilized in keeping these muscles relaxed in the presence of Ca^{2+}.

TnC as a primary target for the W7 inhibition of calcium activation

The W7 inhibition is most likely mediated via specific interactions between W7 and TnC. In solution W7 binds specifically to TnC and not to Tm, actin, or myosin (Hidaka et al., 1980). Significantly, the $K_{\text{I-Tension}}$ values determined here in both muscle types are in excellent agreement with the previously determined K_D of 25 μM of W7 for TnC in solution (Hidaka et al., 1980), strongly supporting the notion that TnC is the primary target for the W7 inhibition.

Recent NMR studies show one molecule of W7 bound to one domain of CaM, competing directly for the deep hydrophobic pocket where the CaM-activated regulatory proteins bind (Osawa et al., 1998). Since the 10 N-terminal residues of CaM involved in the W7 binding differ from TnC by only one conservative substitution in fast skeletal TnC (Ile-60 in place of Met-52 of CaM (Huang et al., 1998; Osawa et al., 1998) and mouse cardiac TnC (Val-73 in place of Ile-64) (our unpublished data), it is likely that W7 binds to TnC in the same way. Additionally, since the overall conformation and the recognition mechanisms are similar between the structures of TnC/TnI1-47 (Vassylyev et al., 1998) and CaM-target peptides (Ikura et al., 1992; Meador et al., 1992), we speculate that W7 might competitively inhibit the interactions between TnI and TnC during calcium activation, thereby disabling the thin filaments (see Scheme 1 below).

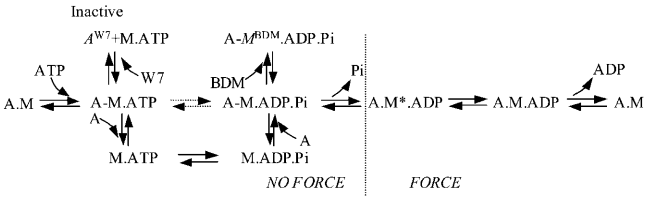

The possibility that inhibition results from TnC extraction is unlikely, in view of the rapid and reversible action of W7. Furthermore, our tension-pCa data at varying W7 concentrations in skeletal muscle fibers are in excellent general agreement with recent studies where native TnC was replaced with varying amounts of nonfunctional TnC (Regnier et al., 2002), suggesting an inactive TnC upon W7 binding. Other secondary targets of W7, such as myosin light chains and other EF hand proteins are conceivable, but unlikely to be quantitatively significant. Solution ATPase activities of myosin and actomyosin are not significantly altered when light chains (RLC or ELC) are chemically modified by spin labels attached to their cysteine residues (Adhikari et al., 1997; Palm et al., 1999). Even an ~50% removal of RLC only reduced maximal tension by 20% in rabbit psoas fibers, (Roopnarine, 2003). Our own studies showed a slight inhibitory effect of W7 on the in vitro motility of actin over myosin-heavy meromyosin (e.g., a 25% reduction at 100 μM W7), whereas the high salt Ca^{2+} and Mg^{2+} S1 ATPase activities were unaffected up to 300 μM W7 (B. Adhikari, W. Li, and K. Wang, unpublished observations). These biochemical data suggest a possible inhibition of actomyosin interaction, albeit at high concentrations of W7. Another potential candidate, S100A1, a calcium sensor protein that modulates skeletal and cardiac muscle activation (Adhikari and Wang, 2001; Most et al., 2001), is absent in the skinned muscle fibers used (B. Adhikari and K. Wang, unpublished observations). S100A1 therefore is not a relevant target of W7 in these skinned fibers.

Calcium activation: an interplay of the thin and the thick filaments

Based on the analysis above, a scheme of the inhibitory action of W7 in the context of an actomyosin chemomechanical cycle (from Tesi et al., 2002) is presented in Scheme 1 (*A*, actin-thin filament; *M*, myosin; all inactivated forms are in italic). During activation of untreated fibers, Ca^{2+} binds and activates TnC, which in turn activates the thin filaments, enabling myosin to interact with actin, to hydrolyze ATP and to generate force (noforce-to-force transition). W7 is proposed to bind primarily to the Ca^{2+} bound form of TnC and inactivates the thin filament (A^{W7} in Scheme 1) without altering the binding affinity between calcium and TnC (Hidaka et al., 1980; Inagaki et al., 1983). BDM is depicted as inhibiting primarily the A-M.ADP.Pi state, although other states may be secondary targets (Tesi et al., 2002, and references cited therein).

Although a quantitative analysis of this molecular scheme is beyond the scope of this work, some interesting inferences can be reached. First, since W7 appears to inhibit overall ATPase and tension both competitively and noncompetitively (as revealed by its reduction of both pK and maximal activation), we suggest that calcium binding to TnC and the level of activation of the thin filaments are influenced by the subsequent steps in the cycle. A purely noncompetitive inhibitor, where both calcium binding to TnC and the level of thin filament activation are independent of subsequent steps (see Eq. 2 in Methods), would reduce ATPase and tension without reducing pK or *n*. Likewise, the mixed-type inhibition for BDM or for BDM plus W7 is consistent with the presence of significant interdependence between the level of activation of the thin filaments and the strength of the actin-myosin interactions.

Current molecular models for activation invoke three states of thin filaments, corresponding to three positions of Tm on the thin filament (al-Khayat et al., 1995; Craig and Lehman, 2001; Lehman et al., 1994; McKillop and Geeves, 1993; Smith and Geeves, 2003; Smith et al., 2003; Vibert et al., 1997). Under relaxing conditions, Tm lies at the periphery of the actin filaments in the *blocked* position whereas myosin heads are largely detached. With the rise in calcium ions, Tm shifts to the *closed* state, where weak interactions are allowed between myosin heads and thin filament, and then to the *open* state where strong interactions occur and generate force. The calcium-dependent transition between the closed and open states of Tm is thought to be the most important step for activation, with the strongly bound myosin heads in the open state contributing to the high cooperativity of activation (reviewed in Gordon et al., 2001; Hitchcock-DeGregori, 2002). A blocked and/or closed Tm position, where myosin heads are unable to strongly attach to thin filaments and generate force, would be consistent with the proportional inhibition of tension and stiffness inhibition by W7 (Fig. 3, *inset*).

It is thought that the level of force during Ca^{2+} activation reflects the availability of open Tm states (Gordon et al., 2000). The observation that W7 and BDM either interfere each other at high pCa (level of force is higher than predicted sum) or enhance each other at low pCa (level of force is lower than the predicted sum) suggests a complex, calcium-dependent redistribution of Tm states when both pathways are inhibited. Our data thus support and extend the notion that calcium activation of striated muscle contractility involves an interplay between the activation of regulatory complexes of the thin filament and the binding and cycling of myosin heads to thin filaments, as previously proposed by others (Fitzsimons et al., 2001; Fuchs, 1977; Gordon et al., 1988; Guth and Potter, 1987; Hoar et al., 1987; Li and Fajer, 1994, 1998; Millar and Homsher, 1990; Swartz and Moss, 1992; Wakabayashi et al., 1991). W7 inhibition provides a glimpse of the additional complexity of the calcium regulation pathways and it can be exploited, either alone or in combination with other effectors, to achieve a more quantitative understanding of the elementary steps of calcium activation pathways, especially the interdependence of the various steps (see e.g., Razumova et al., 2000).

Tension cost and calcium activation of skeletal and cardiac muscles

The tension cost as a function of calcium activation can be examined in terms of a simple two-state model of force generation based on the original 1957 Huxley model (Huxley, 1957), where myosin heads switch between the nonforce generating (weak) and force generating (strong) states and hydrolyze one molecule of ATP per cycle (reviewed in Sieck and Regnier, 2001). The transition between the two groups of states can be described by f_{app}, the forward rate constant, and g_{app}, the reverse rate constant (Brenner, 1988; Kerrick et al., 1991; Kushmerick and Krasner, 1982). In this model the ratio of ATPase/tension equals the product of the number of half sarcomeres in the fiber, the mean force generated by each myosin head (F) and g_{app}. Since the number of half sarcomeres is constant for the same sample, the changes of this ratio reflect changes of F, g_{app}, or both.

The declining ATPase/tension ratio with increasing activation level implies a decrease in either the mean force of myosin head and/or in the rate of myosin head dissociation. Conversely, the higher ratio during inhibition over the entire pCa range (Fig. 8) implies increased myosin mean force and/or higher myosin head dissociation rate (i.e., more myosin heads in the weak-binding states). It should be noted that the experimental error in the ATPase/tension ratio is substantial for the region near the onset of activation. However, this error quickly declines as tension increases and approaches the maximum. For this reason, comparison of tension cost-pCa curves are more useful at pCa below the midpoint of the activation, which is ~5.6 for skeletal muscle and ~5.4 for cardiac fibers (see Fig. 8). The presence of the leading component of ATPase curves between pCa 6.6 and 5.8 (*brackets* in Fig. 4) contributed at least partly to the high tension cost near pCa 5.8–5.6. Interestingly, this leading component is absent in the cardiac muscle and the tension cost curve is independent of pCa. These data raise the possibility that this inhibitor-sensitive component of ATPase of skeletal muscle reflects the existence of a heretofore-uncharacterized calcium sensitive actomyosin interaction between pCa 6.6 and 5.8.

The tension cost-pCa curves reveal that the mouse cardiac tissue is more efficiently coupled for tension generation over the entire range of activation, whereas skeletal muscle appears to be at maximum efficiency only at or near maximal activation. It may be no coincidence that energy efficiency is somehow optimized to coincide with the range of their physiological levels of activation, which is submaximal for cardiac fibers and maximal for skeletal fibers (Fabiato, 1981). The interplay of the two activation pathways may play a role in the mechanism of optimization of energy-tension coupling.

In summary, we have presented a novel use of W7 to reversibly inhibit striated muscle activation. This inhibition appears to act primarily via the binding to TnC and the subsequent inactivation of the thin filaments. Examination of the tension and ATPase curves over the entire range of calcium activation in the presence of W7, BDM, and a combination of both, have revealed the complexity and interplay of thin filament- and thick filament-based activation pathways.

We thank Glenn Kerrick for consultation on the Guth instrument, and La Shaun Berrien and April Adhikari for critical reading of the manuscript. We thank the anonymous reviewers for their insights.

REFERENCES

Adhikari, B., K. Hideg, and P. G. Fajer. 1997. Independent mobility of catalytic and regulatory domains of myosin heads. *Proc. Natl. Acad. Sci. USA.* 94:9643–9647.

Adhikari, B. B., and K. Wang. 2001. S100A1 modulates skeletal muscle contraction by desensitizing calcium activation of isometric tension, stiffness and ATPase. *FEBS Lett.* 497:95–98.

al-Khayat, H. A., N. Yagi, and J. M. Squire. 1995. Structural changes in actin-tropomyosin during muscle regulation: computer modeling of low-angle x-ray diffraction data. *J. Mol. Biol.* 252:611–632.

Allen, K., Y. Y. Xu, and W. G. Kerrick. 2000. Ca^{2+} measurements in skinned cardiac fibers: effects of Mg^{2+} on Ca^{2+} activation of force and fiber ATPase. *J. Appl. Physiol.* 88:180–185.

Bagshaw, C. R. 1993. Muscle Contraction. Chapman & Hal, London and New York.

Brenner, B. 1988. Effect of Ca^{2+} on cross-bridge turnover kinetics in skinned single rabbit psoas fibers: implications for regulation of muscle contraction. *Proc. Natl. Acad. Sci. USA.* 85:3265–3269.

Cheung, A., J. A. Dantzig, S. Hollingworth, S. M. Baylor, Y. E. Goldman, T. J. Mitchison, and A. F. Straight. 2002. A small-molecule inhibitor of skeletal muscle myosin II. *Nat. Cell Biol.* 4:83–88.

Craig, R., and W. Lehman. 2001. Crossbridge and tropomyosin positions observed in native, interacting thick and thin filaments. *J. Mol. Biol.* 311:1027–1036.

Donaldson, S. K., and W. G. Kerrick. 1975. Characterization of the effects of Mg^{2+} on Ca^{2+}- and Sr^{2+}-activated tension generation of skinned skeletal muscle fibers. *J. Gen. Physiol.* 66:427–444.

Fabiato, A. 1981. Myoplasmic free calcium concentration reached during the twitch of an intact isolated cardiac cell and during calcium-induced release of calcium from the sarcoplasmic reticulum of a skinned cardiac cell from the adult rat or rabbit ventricle. *J. Gen. Physiol.* 78:457–497.

Fewell, J. G., T. E. Hewett, A. Sanbe, R. Klevitsky, E. Hayes, D. Warshaw, D. Maughan, and J. Robbins. 1998. Functional significance of cardiac myosin essential light chain isoform switching in transgenic mice. *J. Clin. Invest.* 101:2630–2639.

Fitzsimons, D. P., J. R. Patel, K. S. Campbell, and R. L. Moss. 2001. Cooperative mechanisms in the activation dependence of the rate of force development in rabbit skinned skeletal muscle fibers. *J. Gen. Physiol.* 117:133–148.

Fuchs, F. 1977. Cooperative interactions between calcium-binding sites on glycerinated muscle fibers. The influence of cross-bridge attachment. *Biochim. Biophys. Acta.* 462:314–322.

Gordon, A. M., E. Homsher, and M. Regnier. 2000. Regulation of contraction in striated muscle. *Physiol. Rev.* 80:853–924.

Gordon, A. M., M. Regnier, and E. Homsher. 2001. Skeletal and cardiac muscle contractile activation: tropomyosin ''rocks and rolls''. *News Physiol. Sci.* 16:49–55.

Gordon, A. M., E. B. Ridgway, L. D. Yates, and T. Allen. 1988. Muscle cross-bridge attachment: effects on calcium binding and calcium activation. *Adv. Exp. Med. Biol.* 226:89–99.

Granzier, H. L., and K. Wang. 1993. Passive tension and stiffness of vertebrate skeletal and insect flight muscles: the contribution of weak cross-bridges and elastic filaments. *Biophys. J.* 65:2141–2159.

Guth, K., and J. D. Potter. 1987. Effect of rigor and cycling cross-bridges on the structure of troponin C and on the Ca^{2+} affinity of the Ca^{2+}-specific regulatory sites in skinned rabbit psoas fibers. *J. Biol. Chem.* 262:13627–13635.

Herrmann, C., J. Wray, F. Travers, and T. Barman. 1992. Effect of 2,3-butanedione monoxime on myosin and myofibrillar ATPases. An example of an uncompetitive inhibitor. *Biochemistry.* 31:12227–12232.

Hidaka, H., T. Yamaki, M. Naka, T. Tanaka, H. Hayashi, and R. Kobayashi. 1980. Calcium-regulated modulator protein interacting agents inhibit smooth muscle calcium-stimulated protein kinase and ATPase. *Mol. Pharmacol.* 17:66–72.

Hilber, K., Y. B. Sun, and M. Irving. 2001. Effects of sarcomere length and temperature on the rate of ATP utilisation by rabbit psoas muscle fibres. *J. Physiol.* 531:771–780.

Hitchcock-DeGregori, S. E. 2002. Tropomyosin. *In* Encyclopedia of Molecular Medicine. T. Creighton, editor. John Wiley and Sons, New York. 3247–3251.

Hoar, P. E., C. W. Mahoney, and W. G. Kerrick. 1987. $MgADP^{-}$ increases maximum tension and Ca^{2+} sensitivity in skinned rabbit soleus fibers. *Pflugers Arch.* 410:30–36.

Huang, W., G. J. Wilson, L. J. Brown, H. Lam, and B. D. Hambly. 1998. EPR and CD spectroscopy of fast myosin light chain conformation during binding of trifluoperazine. *Eur. J. Biochem.* 257:457–465.

Huxley, A. F. 1957. Muscle structure and theories of contraction. *Prog. Biophys. Biophys. Chem.* 7:255–318.

Ikura, M., G. M. Clore, A. M. Gronenborn, G. Zhu, C. B. Klee, and A. Bax. 1992. Solution structure of a calmodulin-target peptide complex by multidimensional NMR. *Science.* 256:632–638.

Inagaki, M., T. Tanaka, and H. Hidaka. 1983. Calmodulin antagonists enhance calcium binding to calmodulin. *Pharmacology.* 27:125–129.

Kerrick, W. G., J. D. Potter, and P. E. Hoar. 1991. The apparent rate constant for the dissociation of force generating myosin crossbridges from actin decreases during Ca^{2+} activation of skinned muscle fibres. *J. Muscle Res. Cell Motil.* 12:53–60.

Kushmerick, M. J., and B. Krasner. 1982. Force and ATPase rate in skinned skeletal muscle fibers. *Fed. Proc.* 41:2232–2237.

Lehman, W., R. Craig, and P. Vibert. 1994. Ca^{2+}-induced tropomyosin movement in *Limulus* thin filaments revealed by three-dimensional reconstruction. *Nature.* 368:65–67.

Li, H. C., and P. G. Fajer. 1994. Orientational changes of troponin C associated with thin filament activation. *Biochemistry.* 33:14324–14332.

Li, H. C., and P. G. Fajer. 1998. Structural coupling of troponin C and actomyosin in muscle fibers. *Biochemistry.* 37:6628–6635.

Martell, A. E., and R. M. Smith. 1974. Critical Stability Constants. Plenum Press, New York.

Martyn, D. A., C. J. Freitag, P. B. Chase, and A. M. Gordon. 1999. Ca^{2+} and cross-bridge-induced changes in troponin C in skinned skeletal muscle fibers: effects of force inhibition. *Biophys. J.* 76:1480–1493.

McKillop, D. F., N. S. Fortune, K. W. Ranatunga, and M. A. Geeves. 1994. The influence of 2,3-butanedione 2-monoxime (BDM) on the interaction between actin and myosin in solution and in skinned muscle fibres. *J. Muscle Res. Cell Motil.* 15:309–318.

McKillop, D. F., and M. A. Geeves. 1993. Regulation of the interaction between actin and myosin subfragment 1: evidence for three states of the thin filament. *Biophys. J.* 65:693–701.

Meador, W. E., A. R. Means, and F. A. Quiocho. 1992. Target enzyme recognition by calmodulin: 2.4 Å structure of a calmodulin-peptide complex. *Science.* 257:1251–1255.

Millar, N. C., and E. Homsher. 1990. The effect of phosphate and calcium on force generation in glycerinated rabbit skeletal muscle fibers. A steady-state and transient kinetic study. *J. Biol. Chem.* 265:20234–20240.

Most, P., J. Bernotat, P. Ehlermann, S. T. Pleger, M. Reppel, M. Borries, F. Niroomand, B. Pieske, P. M. Janssen, T. Eschenhagen, P. Karczewski, G. L. Smith, W. J. Koch, H. A. Katus, and A. Remppis. 2001. S100A1: a regulator of myocardial contractility. *Proc. Natl. Acad. Sci. USA.* 98:13889–13894.

Ogawa, Y., and N. Kurebayashi. 1989. Modulations by drugs of the relationship between calcium binding to troponin C and tension. *Prog. Clin. Biol. Res.* 315:75–86.

Osawa, M., M. B. Swindells, J. Tanikawa, T. Tanaka, T. Mase, T. Furuya, and M. Ikura. 1998. Solution structure of calmodulin-W-7 complex: the basis of diversity in molecular recognition. *J. Mol. Biol.* 276:165–176.

Palm, T., K. Sale, L. Brown, H. Li, B. Hambly, and P. G. Fajer. 1999. Intradomain distances in the regulatory domain of the myosin head in prepower and postpower stroke states: fluorescence energy transfer. *Biochemistry.* 38:13026–13034.

Razumova, M. V., A. E. Bukatina, and K. B. Campbell. 2000. Different myofilament nearest-neighbor interactions have distinctive effects on contractile behavior. *Biophys. J.* 78:3120–3137.

Regnier, M., C. Morris, and E. Homsher. 1995. Regulation of the cross-bridge transition from a weakly to strongly bound state in skinned rabbit muscle fibers. *Am. J. Physiol.* 269:C1532–C1539.

Regnier, M., A. J. Rivera, C. K. Wang, M. A. Bates, P. B. Chase, and A. M. Gordon. 2002. Thin filament near-neighbour regulatory unit interactions affect rabbit skeletal muscle steady-state force-Ca^{2+} relations. *J. Physiol.* 540:485–497.

Roopnarine, O. 2003. Mechanical defects of muscle fibers with myosin light chain mutants that cause cardiomyopathy. *Biophys. J.* 84:2440–2449.

Sieck, G. C., and M. Regnier. 2001. Invited review: Plasticity and energetic demands of contraction in skeletal and cardiac muscle. *J. Appl. Physiol.* 90:1158–1164.

Smith, D. A., and M. A. Geeves. 2003. Cooperative regulation of myosin-actin interactions by a continuous flexible chain. II. Actin-tropomyosin-troponin and regulation by calcium. *Biophys. J.* 84:3168–3180.

Smith, D. A., R. Maytum, and M. A. Geeves. 2003. Cooperative regulation of myosin-actin interactions by a continuous flexible chain I: actin-tropomyosin systems. *Biophys. J.* 84:3155–3167.

Swartz, D. R., and R. L. Moss. 1992. Influence of a strong-binding myosin analogue on calcium-sensitive mechanical properties of skinned skeletal muscle fibers. *J. Biol. Chem.* 267:20497–20506.

Tesi, C., F. Colomo, N. Piroddi, and C. Poggesi. 2002. Characterization of the cross-bridge force-generating step using inorganic phosphate and BDM in myofibrils from rabbit skeletal muscles. *J. Physiol.* 541:187–199.

Vassylyev, D. G., S. Takeda, S. Wakatsuki, K. Maeda, and Y. Maeda. 1998. Crystal structure of troponin C in complex with troponin I fragment at 2.3-Å resolution. *Proc. Natl. Acad. Sci. USA.* 95:4847–4852.

Vibert, P., R. Craig, and W. Lehman. 1997. Steric-model for activation of muscle thin filaments. *J. Mol. Biol.* 266:8–14.

Wakabayashi, K., H. Tanaka, H. Saito, N. Moriwaki, Y. Ueno, and Y. Amemiya. 1991. Dynamic x-ray diffraction of skeletal muscle contraction: structural change of actin filaments. *Adv. Biophys.* 27:3–13.

Wang, Y., Y. Xu, K. Guth, and W. G. Kerrick. 1999. Troponin C regulates the rate constant for the dissociation of force-generating myosin cross-bridges in cardiac muscle. *J. Muscle Res. Cell Motil.* 20:645–653.

Zhao, L., N. Naber, and R. Cooke. 1995. Muscle cross-bridges bound to actin are disordered in the presence of 2,3-butanedione monoxime. *Biophys. J.* 68:1980–1990.

Zhao, Y., and M. Kawai. 1994. BDM affects nucleotide binding and force generation steps of the cross-bridge cycle in rabbit psoas muscle fibers. *Am. J. Physiol.* 266:C437–C447.